Proceedings of the International Seminar on Mineral Processing Technology - 2006, Chennai, India. pp. 203 - 209.

CFD Simulation Studies on a 19^0 Cone Angle Hydrocyclone

K. Udaya Bhaskar[1], Y. Rama Murthy[1], J.K. Srivastava[2] and N. Ramakrishnan[1]

[1] *Regional Research laboratory, Hoshangabad Road, Bhopal – 462026*
Corresponding author Email: kubhaskar2001@yahoo.com
[2] *Chemical Engineering Department, Ujjain Engineering College, Ujjain - 456001*

Abstract

Hydrocyclone being in practice for classification applications are of low cone angle typically at 10^o. The details on the simulation of such hydrocyclone are well reported. The present study is an attempt to simulate the water flow behaviour inside a 3 inch 19^0 cone angle hydrocyclone, which in general is applied for processing intermediate size coal and is popularly know as heavy medium cyclone. A 3D axi-symmetric model of standard 3" heavy medium cyclone geometry is generated. The computational domain is divided into unstructured grid having 115053 tetrahedral volumes using GAMBIT preprocessor. A segregated solver with steady state 3-D double precision scheme was used for model computations assigning a convergence value of 1e-06. For predicting swirling flow characteristics prevailing inside the cyclone, Pressure Interpolation Scheme (PRESTO) is used. Reynolds stress model (RSM), which was reported to account with greater precision for the effects of swirl, rotation etc. was selected for turbulence calculations. For obtaining the pressure field inside the system SIMPLE algorithm scheme was used. Higher-order Quadratic Upwind Interpolation (QUICK) spatial discretisation scheme was used for field variables interpolation from cell centers to faces of the control volumes. Tangential, axial velocity profiles and pressure distributions are presented and the water-split values obtained through simulation are compared with the experimental results.

Keywords: *Hydrocyclone, CFD, velocity profiles, water splits.*

INTRODUCTION

Hydrocyclones are one of the well-established classifying units in the processing industry. These units are employed for classification of minerals and materials in a wide range of industries pertaining to mineral processing, chemical engineering etc. Due to several advantages, such as ease of operation, high throughput, less maintenance, less floor space requirement etc., hydrocyclones have been widely accepted in the area of mineral processing. Though hydrocyclone was patented in late 18^{th} century, rigorous understanding on principles and application began only in mid fifties [Kelsall (1952, 1953)]. These studies of Kelsall on the axial, radial and tangential velocity profiles inside a cyclone formed the basis for the subsequent research. Due to several prohibiting conditions, like complex nature of the phenomenon involved, non-availability of high-speed computational systems etc., most of the research work till recent times was focused on the empirical modeling [Lynch and Rao (1975); Plitt (1976)]. With the advent of high speed computational systems, in the recent past, significant work has been reported on the simulation of hydrocyclone performance using Computational Fluid Dynamics (CFD) techniques [Hsieh and Rajamani (1986); Monredon et al. (1991); Rajamani and Milin (1992); Slack and Wraith (1997); Stovin and Saul (1998); Slack et.al., (2000); Slack and Wraith (2002); Grady et.al., (2002); Slack et.al (2003); Schuetz et.al.,(2003); Grady et.al., (2003)].

MODEL DESCRIPTION

Geometry

The hydrocyclone geometry used for simulation studies is presented in Fig. 1. The geometry consists of a main cylindrical body with 76mm diameter and 80 mm in length. A frustum with top diameter of 76 mm and with bottom diameter of 13mm maintained at a cone angle of 19° is connected to the main cylindrical body. Studies were carried out by changing the bottom diameter of the frustum to 13, 17 mm and vortex finder diameter to 19, 22, 25mm at a constant cone angle of 19°. A cylindrical vortex finder with an inner diameter of 25 mm and outer diameter of 40 mm protrudes into the main cylindrical body extending over a length of 60 mm inside and 37 mm above the top surface. A rectangular tangential feed inlet opening is connected to the cylindrical surface at a height of 15 mm below the top surface.

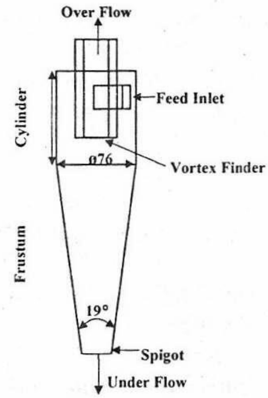

Fig. 1: Hydrocyclone Geometry

Meshing Scheme

Hydrocyclones are not axisymmetric at the feed inlet opening and therefore it is not appropriate to model the geometry in a 2-D plane. Also, the results of the earlier researchers using a 3-D model are reported to have better agreement with the experimental data compared to that of an analysis assuming axisymmetric geometry. [www.psl.bc.ca/downloads/ presentations/cyclone/cyclone.html]. Thus in the present study, simulations were carried out to understand the flow behaviour of water using a 3-D computational model. A mesh density of 115053 computational cells was used as an optimum value for further studies on the variables. A fully unstructured grid based on tetrahedral cells with T-grid meshing scheme was used for describing the cyclone geometry

Boundary and Initial Conditions

The cyclone body consists of an inlet for feed and two outlets for products discharge, termed as overflow and underflow. Feed inlet was designated as pressure inlet. The overflow and underflow outlets were defined as pressure outlets. Water was fed into the cyclone as a primary phase with density 998.2kg/m^{3}and a viscosity value of 0.001003kg/m-s. Water pressure inlet values of 68947.57 Pascal (10 psi) were defined. The underflow outlets of 13mm and 17 mm corresponding to the experimental conditions were varied in the simulated geometry.

SIMULATION

Numerical simulations were carried out in Cartesian coordinate system. A segregated steady state 3-D double precision solver was used for simulating the flow conditions. The segregated solver solves the governing Nevier Stokes equations sequentially using iterative methods till the defined values of convergence are met. The properties of the water are used at the beginning along with the pressure and face mass fluxes for calculating the momentum equations and further update the velocity field. PRESTO (Pressure staggered option), a pressure interpolation scheme which is useful for predicting highly swirling flow characteristics prevailing inside the cyclone body [Fluent Europe Ltd (2002)] was adopted. Further, Reynolds stress model (RSM), which was reported to account with greater precision for the effects of streamline curvature, swirl, rotation, and rapid changes in strain rate with anisotropic behavior etc. [Slack, Porte, Engelman (2003)], was selected for turbulence calculations. SIMPLE algorithm scheme, which uses a combination of continuity and momentum equations to derive an equation for pressure, was used for pressure and velocity coupling to obtain the pressure field inside the system [Schuetz, Mayor, Bierdel, Piesche (2003)]. Higher-order Quadratic Upwind Interpolation (QUICK) spatial discretisation scheme reported to be useful for swirling flows was used for field variables interpolation from cell centers to faces of the control volumes [Fluent Europe Ltd (2002)]. Simulations were carried out for about 10,000 incremental steps where in general a preset value of convergence criteria 1e-06 was achieved

EXPERIMENTAL

The test rig (Figure 2) used for carrying out the experimental work consists of a feed slurry tank of 200 liters capacity mounted on a stable platform. The bottom of the feed tank was connected to a centrifugal pump driven by a 3-phase, 5.5 kW motor. The outlet of the pump was connected to the feed inlet of a 76mm hydrocyclone. A by-pass pipe with a control valve was connected to the pump outlet line to maintain the required pressure drop inside the cyclone. A diaphragm type pressure gauge was fitted near the feed inlet to indicate the pressure drop. The hydrocyclone was positioned vertically above the slurry tank. In the experimental design, the levels of spigot opening and vortex finder diameter were selected to generate a wide range of water splits into the overflow and underflow products. Required size vortex finder and spigot as per the experimental design was fitted to the cyclone after fixing the main body to the test-rig. In the water-distribution studies, water was pumped into the cyclone at different vortex finder diameter and spigot openings. Timed samples of overflow and underflow products were collected separately.

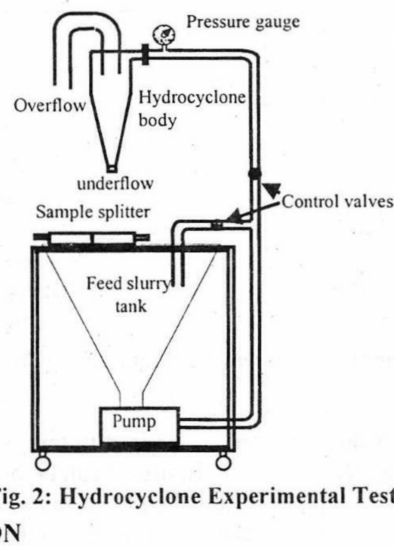

Fig. 2: Hydrocyclone Experimental Test-Rig

RESULTS AND DISCUSSION

While treating water in the cyclone, information on the cyclone water-split (percent report of total water entering the cyclone) into overflow product were used for validating the predictions at different test runs with the experimental values. The simulation studies were carried out using standard

Reynolds Stress Model at three different vortex finder openings, i.e. 19mm, 22mm, and 25mm and two different spigot openings i.e., 13mm and 17mm. All these simulations were carried out at a constant feed inlet pressure of 68947.5 Pascal (10psi). The results obtained are discussed in two stages. Initial discussions cover the simulated general flow patterns in the cyclone in terms of velocity and static pressure. Later, comparison of simulated results obtained interms of water spilt to over flow are discussed specifically validating with the experimental results.

General Flow Behavior

The general flow behavior in terms of velocity distributions at different planes inside the system are discussed with qualitative comparison of the published flow profiles of hydrocyclones [Hsieh and Rajamani (1986); Slack and Wraith (2002); Fluent Europe Ltd (2002); Slack et.al., (2003)]

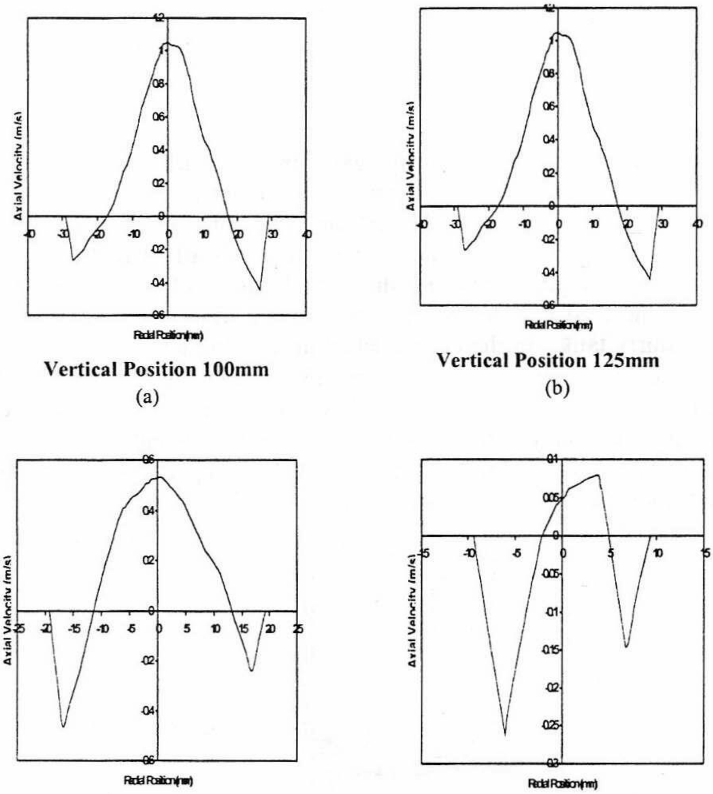

Vertical Position 100mm
(a)

Vertical Position 125mm
(b)

Vertical Position 175mm
(c)

Vertical Position 225mm
(d)

Fig. 3: Axial Velocity at Different Vertical Positions Inside the Cyclone

Axial Velocity

The results obtained on the axial velocity distributions in different X-Y planes at different positions, are shown in Fig. 3(a) through Fig. 3(d). From the figures it can be observed that a maximum positive axial velocity values indicating a vertically upward flow exists at or very near the cyclone axis. With the increasing radial distance, this value decreases till it reaches zero at some distance away from the cyclone axis. With a further increase in the radial distance, negative axial velocity indicating a vertically downward flow begins. This observation can be made at all the heights inside the conical body. A maximum negative axial velocity was observed at some radial distance away from the cyclone wall. A comparison of these figures also indicates that the peak value of positive axial velocity is maximum immediately below the bottom of the vortex finder (Fig. 3(a)) and minimum at or near the spigot opening (Fig. 3(d)).

Contours of axial velocities along vertical and radial planes are presented Fig. 4(a) and Fig. 4(b). The figures indicate that along the cyclone height there are concentric layers of similar axial velocities. The figures also indicate both the positive and negative axial velocity profiles.

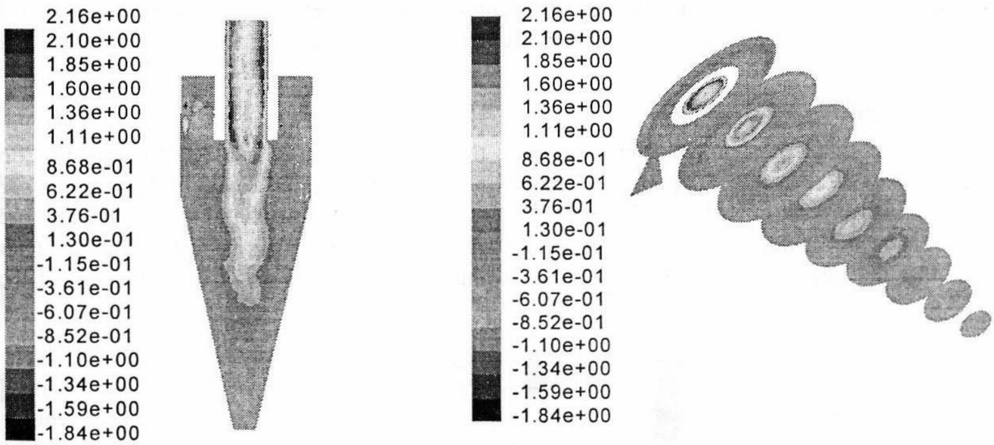

(A) **(B)**

Fig. 4: (A) Contours of Axial Velocity (M/Sec) in Vertical Plane, (B) Contours of Axial Velocity (M/Sec) in Horizontal Planes

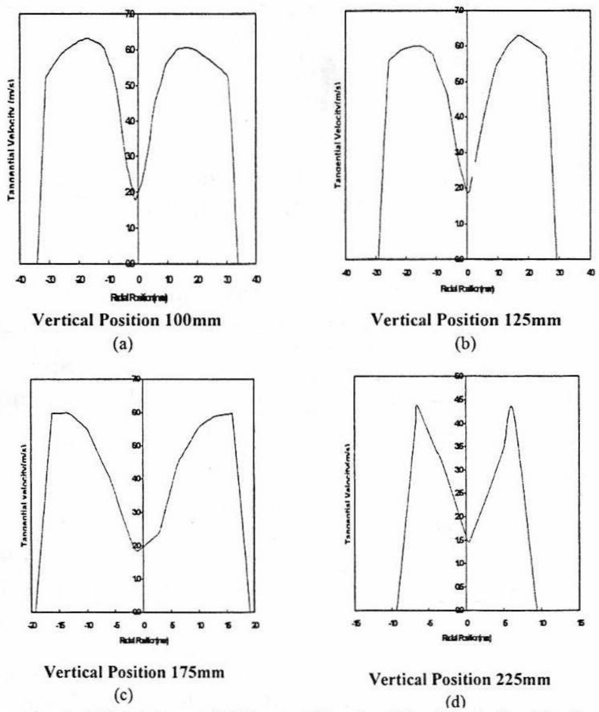

Vertical Position 100mm
(a)

Vertical Position 125mm
(b)

Vertical Position 175mm
(c)

Vertical Position 225mm
(d)

Fig. 5: Tangential Velocity at Different Vertical Positions Inside the Cyclone

Tangential Velocity

The tangential velocities of the simulated results in X-Y planes at different vertical positions are shown in Fig. 5(a) to Fig. 5(d). The figures indicate that the tangential velocity initially increases with the radial positions till a particular value and then decreases. The published reports [Monredon et al. (1991); Slack et al. (2002)] also indicate that the tangential velocity increases sharply with radius in the central core region under the vortex finder and that thereafter decreases with radius. A comparison of the figures indicate that the tangential velocity pattern remains more or less similar while the values for maximum tangential velocity decrease with increase in the axial distances of the cyclone body.

Pressure Distribution

The contours of static pressure distribution inside the hydrocyclone in axial and radial direction are presented in Figure 6(a) and 6(b) respectively. The Figure shows that a negative static pressure has generated at the core section. As the hydrocyclone is open to atmosphere this negative static pressure causes a suction of air due to which an air core forms along the axis of the cyclone. Further it may be observed that the intensity of pressure increases along radial direction and maximum at near the feed inlet.

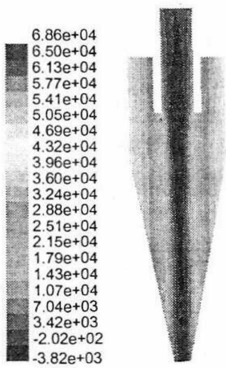

(a)

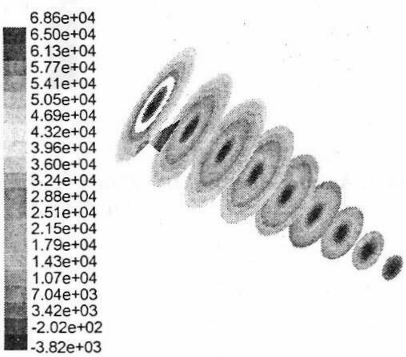

(b)

Fig. 6: (A) Contours of Static Pressure (Pascal) Along Vertical Plane, (B): Contours of Static Pressure (Pascal) Along Horizontal Planes

Validation Results

The result obtained on the water split under experimental conditions is compared with the simulated results. The results are presented in table 1. **Table 1: Experimental and Simulated Results of Water Split**

			% Split to OF		
Sl. No.	VFD (mm)	SPD (mm)	Experimental	Simulated	% Error
1.	19	13	82.26	84.34	2.53
2.	22	13	84.34	80.68	-4.34
3.	25	13	95.93	93.80	-2.22
4.	19	17	47.26	45.39	-3.96
5.	22	17	71.60	77.92	8.83
6.	25	17	85.41	78.39	-8.22

Water Split

Water split in hydrocyclone is defined as the percentage of the water throughput reporting to over flow. The simulated results obtained were compared with the experimental data and are presented in Table 1. It can be observed from the table that the simulated results of water split are found closely matching with the experimental values. The percentage errors were observed to be in a range of 2.22% to 8.82%.

CONCLUSIONS

A CFD simulation and supporting validation study on 3 inch 19^0 cone angle hydrocyclone have demonstrated the applicability in the analysis of the water splits for various test conditions. The simulation results on water split have found matching with the experimental results with a reasonable accuracy.

REFERENCES

[1] Fluent Europe Ltd. (2002): D30-1_TAR_P32_AC - Cyclone separator. Thematic area 3, http//www.qnet-cfd.net.

[2] Fluent Inc. (2002): Modeling Turbulence, Fluent 6.0 documentation, 10.43 – 10.52.

[3] Grady, S. A.; Wesson, G. D.; Abdullah, M. M.; Kalu, E. E. (2002): Prediction of flow field in 10-mm hydrocyclone using computational fluid dynamics, Fluid and Particle Separations Journal, ,14, 1 – 11.

[4] Grady, S.A.; Wesson, G.D.; Abdullah, M.M.; Kalu, E.E. (2003): Prediction of 10 mm hydrocyclone separation efficiency using computational fluid dynamics, Research article, Dept. of Chemical and Civil Engineering, FAMU-FSU College of Engineering, Tallahassee, and USA.

[5] Hsieh, K. T.; Rajamani, K. (1986): Phenomenological model of the hydrocyclone: Model development and verification for single-phase flow, International Journal of Mineral Processing, 22,1-4,223-237.

[6] Kelsall, D. F. (1952): A study of the motion of solid particles in a hydraulic cyclone. Transactions, Institute Chemical Engineers, 30, 87-108.

[7] Kelsall, D. F. (1953): A further study on hydraulic cyclone. Chemical Engg. Sci., 2, 254-272.

[8] Lynch, A. J.; Rao, T.C. (1975): Modelling and scale up of hydrocyclone classifiers. Proc. Int. Miner. Process. Congr., 11, Cagliari, 245-269.

[9] Monredon, T.C.; Hsieh, K.T.; Rajamani, R.K. (1992): Fluid flow model of the hydrocyclone: an investigation of device dimensions, International Journal Mineral Processing, 35, 1-2,65-83.

[10] Plitt, L.R. (1976): A mathematical model of the hydrocyclone classifier. CIM Bull., 116.

[11] Rajamani, R. K.; Milin, L. (1992): Fluid flow model of the hydrocyclone for concentrated slurry classification. Hydrocyclones: Analysis and Application: 4th Intentional Conference, 12, 95-108.

[12] Schuetz, S.; Mayor, G.; Bierdel, M.: Piesche, M. (2004): Investigations on the flow and separation behavior of hydrocyclones using computational fluid dynamics, International Journal of Mineral Processing, 73,2-4,229-237.

[13] Slack, M. D.; Wraith, A.E. (1997): Modelling the Velocity Distribution in a Hydrocyclone. 4th International Colloquium on Process Simulation, 65-83.

[14] Slack, M.D.; Prasad, R.; Baker, A.; Boysan, F. (2000): Advances in cyclone modelling using unstructured grids, Transactions Institute Chemical Engineers, 78, 1098-1104.

[15] Slack, M.D.; Wraith, A.E. (1997): Modelling the velocity distribution in a hydrocyclone. Dept. Mechanical, Materials and Manufacturing Engineering, University of Newcastle Upon Tyne., BIB 218.

[16] Slack, M. D.; Porte, S. D.; Engelman, M. S. (2003): Designing Automated Computational Fluid Dynamics Modelling Tools for Hydrocyclone Design, Hydrocyclone 2003.

[17] Stovin, V. R; and Saul, A. J. (1998): A computational fluid dynamics (CFD) particle tracking approach to efficiency prediction, Wat. Sci. Tech. Vol.37, No.1, 285-293.

[18] www.psl.bc.ca/downloads/presentations/cyclone/cyclone.html